Neurobiology of Disease 193 (2024) 106453

Contents lists available at ScienceDirect

Neurobiology of Disease

journal homepage: www.elsevier.com/locate/ynbdi

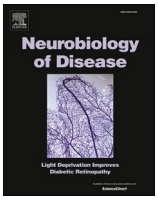

# Gene-environment interaction elicits dystonia-like features and impaired translational regulation in a DYT-TOR1A mouse model

Colette Reinhold [a,1], Susanne Knorr [a,1], Rhonda L. McFleder [a], Lisa Rauschenberger [a], Muthuraman Muthuraman [a], Panagiota Arampatzi [b], Tom Gräfenhan [b], Andreas Schlosser [c], Michael Sendtner [d], Jens Volkmann [a], Chi Wang Ip [a,*]

[a] Department of Neurology, University Hospital of Würzburg, Germany
[b] Core Unit Systems Medicine, Medical Faculty, University Würzburg, Germany
[c] Rudolf Virchow Center for Experimental Biomedicine, University of Würzburg, Germany
[d] Institute of Clinical Neurobiology, University Hospital of Würzburg, Germany

ARTICLE INFO

*Keywords:*
DYT-TOR1A
Multi-omic
Second-hit hypothesis
Dystonia
Nerve injury

ABSTRACT

DYT-TOR1A dystonia is the most common monogenic dystonia characterized by involuntary muscle contractions and lack of therapeutic options. Despite some insights into its etiology, the disease's pathophysiology remains unclear. The reduced penetrance of about 30% suggests that extragenetic factors are needed to develop a dystonic phenotype. In order to systematically investigate this hypothesis, we induced a sciatic nerve crush injury in a genetically predisposed DYT-TOR1A mouse model (DYT1KI) to evoke a dystonic phenotype. Subsequently, we employed a multi-omic approach to uncover novel pathophysiological pathways that might be responsible for this condition. Using an unbiased deep-learning-based characterization of the dystonic phenotype showed that nerve-injured DYT1KI animals exhibited significantly more dystonia-like movements (DLM) compared to naive DYT1KI animals. This finding was noticeable as early as two weeks following the surgical procedure. Furthermore, nerve-injured DYT1KI mice displayed significantly more DLM than nerve-injured wildtype (wt) animals starting at 6 weeks post injury. In the cerebellum of nerve-injured wt mice, multi-omic analysis pointed towards regulation in translation related processes. These observations were not made in the cerebellum of nerve-injured DYT1KI mice; instead, they were localized to the cortex and striatum. Our findings indicate a failed translational compensatory mechanisms in the cerebellum of phenotypic DYT1KI mice that exhibit DLM, while translation dysregulations in the cortex and striatum likely promotes the dystonic phenotype.

## 1. Introduction

The dystonias are rare movement disorders, characterized by involuntary and repetitive movements due to the co-contraction of agonist and antagonist muscles (Albanese et al., 2013). Despite the diversity in etiology, they all share similar clinical symptoms suggesting common affected pathophysiological pathways. The most common hereditary form of dystonia is the DYT-TOR1A dystonia, caused by a glutamic acid deletion (ΔGAG) in the protein product of the*TOR1A* gene. The reduced penetrance of about 30% (Kramer et al., 1994) suggests that the genetic mutation alone might not be sufficient to elicit a dystonic phenotype. This notion is supported by the presence of the same endophenotype in symptomatic and asymptomatic DYT-TOR1A mutation carriers despite divergent clinical manifestation. The endophenotype includes subtle structural changes in the basal ganglia or abnormal synaptic plasticity. (Carbon et al., 2011; Draganski et al., 2009; Edwards et al., 2006). We recently proposed the "second-hit hypothesis", postulating that an additional environmental factor is needed to convert the genetically determined endophenotype into overt dystonia. Several studies have demonstrated the validity of this hypothesis in different dystonia models utilizing a sciatic nerve crush as the environmental stressor enforcing central sensorimotor plasticity mechanisms during recovery. In these studies, animals subjected to the nerve injury exhibited higher dystonia-like movements (DLM) than their naive counterparts (Ip et al., 2016; Knorr et al., 2021; Rauschenberger et al., 2021; Rauschenberger et al., 2021). The abnormal motor phenotype indicates the involvement of the

* Corresponding author at: Josef-Schneider-Straße 11, 97080 Würzburg, Germany.
*E-mail address:* ip_c@ukw.de (C.W. Ip).
[1] These authors contributed equally to this work.

https://doi.org/10.1016/j.nbd.2024.106453
Received 1 December 2023; Received in revised form 17 February 2024; Accepted 22 February 2024
Available online 24 February 2024

basal ganglia, particularly the striatum. However, findings from human and rodent imaging studies, as well as research on symptomatic rodent models, have suggested the engagement of other brain regions. These regions notably include the cortex and the cerebellum. As a result, DYT-TOR1A dystonia is now regarded as a motor network disease rather than solely a basal ganglia disease.

The accessibility of high-throughput technologies has made it possible to study the molecular signature of complex diseases at a large scale, enabling comprehensive insights into their pathophysiological mechanisms. RNA studies conducted on different DYT-TOR1A animal models and cultured cells have demonstrated dysregulations in striatal glutaminergic transmitter system, lipid metabolism, and defects in neuronal development. Additionally, these studies have identified disruption in synaptic plasticity and EIF2α signaling upon the induction of endoplasmic reticulum (ER) stress (Beauvais et al., 2018; Grundmann et al., 2008; Rittiner et al., 2016). While multiple studies have explored the differential gene expression in dystonia, proteomics and microRNA (miRNA) investigations for DYT-TOR1A remain sparse. The available proteome data predominantly utilized PC6–3 inducible torA(wt) and torA(ΔE) cells along with DYT-TOR1A mouse embryonic fibroblast (MEF) cells. These studies showcased the influence of DYT-TOR1A genotype on mitochondrial, metabolic, and stress response pathways (Beauvais et al., 2016; Martin et al., 2009; Shroff et al., 2021). To our knowledge, there has been no study that utilized a high-throughput approach to analyze miRNAs in DYT-TOR1A dystonia. However, altered expressions of several miRNAs have been observed in the peripheral blood of cervical dystonia patients (Gelisin et al., 2023). This underlines the importance of investigating small non coding RNA as potential biomarkers in dystonias, such as DYT-TOR1A dystonia.

To identify the molecules underlying the second-hit response, we induced a sciatic nerve crush injury in DYT1KI mice, which carry the ΔGAG in their endogenous *Tor1a* gene (Goodchild et al., 2005).This injury was able to induce a dystonia-like phenotype in the genetically predisposed animals. We further investigated the impact of the extra-genetic factor in the DYT1KI mice in three relevant brain regions (cortex, striatum, and cerebellum) using an unbiased multi-omics approach (transcriptomic, proteomic and miRNAomic). Our study revealed an impairment in translation-related process in the contralateral cortex and striatum but not in the ipsilateral cerebellum of DYT1KI nerve-injured (crush) mice compared to DYT1KI naive mice. This study identifies the molecular consequences of an environmental trigger on animals with genetic susceptibility. This analysis of long-term molecular effects contributes to our understanding of the intricate interplay between genetics, compensatory and maladaptive network mechanisms and environmental factors in dystonia disorders.

## 2. Materials and methods

### 2.1. Animals

The DYT1 strain (*Tor1a* $^{tm2Wtd}$/J, #025637) was acquired form Jackson lab (Goodchild et al., 2005). A total of 79 male heterozygous DYT1KI mice and 74 male wildtype (wt) littermates, all on C57BL/6 background were bred in the animal facility of the University Hospital of Wuerzburg and kept in standard condition (21 °C, 12-h light/dark cycle). Several cohorts were conducted to ensure standardization of experiments. Mice of the same age (12 weeks old) were selected for each cohort, with distribution of wt and DYT1KI mice varying naturally. Genotype was determined by PCR analysis. Researchers were blinded for the experimental procedure. All animal experiments were approved by the local government and performed in accordance with all applicable international, national, and/or institutional guidelines for care and use of animals.

### 2.2. Sciatic nerve crush injury

A right sciatic nerve crush, as described by Ip et al., 2016 was performed on 12 weeks old, isoflurane and carprofen anesthetized, wt and DYT1KI mice. Briefly, an incision was made on the shaven right hindlimb. The sciatic nerve was exposed and crushed for 1 min using a non-serrated clamp. The incision was subsequently closed, and the animals monitored until fully awake.

### 2.3. Behavioral tests

Behavioral tests were performed at weeks 2, 4, 6, 9, 11 and 12 post nerve crush starting with the preoperative recordings, to assess the severity of the DLM, as well as to analyze the gait of the animals.

#### 2.3.1. Tail suspension test

A tail suspension test (TST) was performed at baseline and at weeks 2, 4, 6, 9, 11 and 12 following the right sciatic nerve crush. Mice were suspended by their tails with the ventral side facing the camera and recorded for two and half minutes. The video recordings were analyzed by a trained deep learning network to evaluate the DLM in the right hindlimb in a computer-based unbiased manner as described previously (Rauschenberger et al., 2023). In brief, DeepLabcut (Mathis et al., 2018) was used to annotate specific body areas to create a deep neural network. This step was performed by two independent investigators in the laboratory not involved in the establishment of the data processing pipeline. The network was trained in 19 iterations on a total of 101 videos from hΔGAG3 mice, DYT1KI mice included in a different project and ΔETorA rats. No animals used in the project herein were included in the training set of the DeepLabCut (DLC) network. For the data processing pipeline, one set of parameters and a deterministic analysis were used across all animals to exclude bias. The network was then used to label our TST videos. The resulting labeled videos were analyzed using a custom software. Videos where the network could not label the right hindlimb with a likelihood of $>$60% in $\geq$50% of frames were excluded from the analysis (wt: 36 videos; DYT1KI: 10 videos). The most common reason was a high amount of hindlimb clasping, which prevented a correct labeling of the right hindlimb. To provide further illustration, we provided DLC-labeled videos showing a DYT1KI naive mice with normal motor behavior (supplementary video S1), a wt crush mice showing some DLM (supplementary video S2), and finally, a DYT1KI crush mice exhibiting multiple DLM (supplementary video S3).

#### 2.3.2. Catwalk XT

Gait analysis was performed using the CatWalk XT (Noldus, Wageningen, Netherlands) at baseline and at weeks 2, 4, 6, 9, 11 and 12 following the right sciatic nerve crush. Mice were placed on the transparent glass walkway and had to cross the runway in a voluntarily manner. The animals' home cage was placed in the goal box to motivate them to walk. At least three compliant runs were recorded, by a camera located underneath the glass plate, for each mouse. A run was considered as compliant when maximum speed variation was lower than 50%, the maximum run duration did not exceed 6 s and the minimum run duration was not shorter than 0.50 s. Only runs where the mice did not stop while crossing the recorded area were analyzed with the Catwalk software (program version 10.6). In this study, a total of 9 parameters Catwalk system were analyzed. (See Table 1.)

### 2.4. Transcriptomics and miRNAomics

Cortex, comprising the primary and secondary motor cortex, primary somatosensory areas and striatum, contralateral to the sciatic nerve crush injury, and cerebellum, ipsilateral to the sciatic nerve crush injury, of naive and nerve-injured mice were microdissected 12 weeks after surgery and put in RNAlater (Invitrogen) for 24 h, before being snap frozen. Total RNA and miRNA isolation was performed using the

**Table 1**
Gait parameters analyzed with Catwalk XT System.

| Parameters | Description |
|---|---|
| Average speed (cm/s) | Average recorded speed of the animal's body during the run |
| RH_Print length (Park et al.) | Horizontal length of the complete print* |
| RH_Print width (Park et al.) | Vertical length of the complete print |
| RH_Max intensityAt (%) | Maximum intensity of the complete print relative to the stand |
| RH_Swing speed (cm/s) | Speed of the paw during the period when there is no contact with the glass surface |
| RH_Step cycle (s) | Time between 2 successive initial contacts of the same paw |
| Step sequence regularity index (%) | Proportion of normal step patterns relative to the overall number of paw placement |
| Phase dispersion RF-RH | Measures the consistency of the paw placement during the animals' walk |
| Coupling RF-RH | Measures the coordination of paws while the animal walks |

* Complete print represents the sum of all paw contact with the glass plate.

miRNeasy micro kit (Qiagen) for the cortex and striatum, and miRNeasy mini kit (Qiagen) for the cerebellum, according to manufacturer's instruction. Library preparation and sequencing were performed by the Core Unit systems medicine, faculty of medicine in Wuerzburg. RNA quality was checked using a 2100 Bioanalyzer with the RNA 6000 Nano kit (Agilent Technologies). The RNA integrity number (RIN) of the total RNA samples was ≥7. DNA libraries suitable for sequencing were prepared from 500 ng of total RNA using the TruSeq Stranded mRNA Library Preparation Kit (Illumina) according to manufacturer's instructions (1/2 volume). After 14 cycles of PCR amplification, the size distribution of the barcoded DNA librariers were eytimated ~320 bp by electrophoresis on Agilent DNA 1000 Bioanalyzer microfluidic chips. 10 ng were used from miRNA-enriched samples and libraries were prepared using QIASeq® miRNA UDI Library Kit. After 18 cycles, the size of the libraries was estimated to 200 bp by electrophoresis on Agilent DNA 1000 Bioanalyzer microfluidic chips. Both miRNA and mRNA were spiked in with 1% PhiX control library and single-end sequencing performed at 16 and 32 Mio. reads/sample respectively, with 100 bp on the NextSeq 2000 platform (Illumina). The files were demultiplexed into FASTQ files, generated with bcl2fastq2 version 2.20.0.422 (Illumina), and checked for quality with FastQC version 0.11.7. Reads obtained from the mRNA sequencing were mapped to the mouse reference genome (GRCm38.p6) and counts were summarized for each gene using featureCounts version 1.6.4 from the Subread package. Mapping and alignment of the reads were performed with STAR version 2.7.2b. Reads generated by the small RNA sequencing were annotated, adapter-trimmed and mapped using miRge3.0 (Patil and Halushka, 2021). The resulting count output of the two RNA sequencing were used to calculate the differentially expressed genes using the DESeq2 Bioconductor/R package. In the cerebellum, the transcriptomic and miRNAomic analyses yielded an average of about 14,468 protein coding genes and 619 unique miRNAs for the DYT1KI crush group, 14,538 genes and 631 miRNAs for the DYT1KI naive group, 14,342 genes and 629 miRNAs for wt crush mice and 14,690 genes and 638 miRNAs for wt naive mice. Similarly in the cortex, the sequencing revealed an average of 14,281 genes and 636 miRNAs in DYT1KI crush animals, 14,110 genes and 653 miRNAs in DYT1KI naive mice, 14,264 genes and 633 miRNAs in wt crush and 14,150 genes and 643 miRNAs for the wt naive group. Lastly, in the striatum the analyses detected 14,129 genes and 655 miRNAs in DYT1KI crush mice, 14,101 genes and 644 miRNAs in the DYT1KI naive group, 14,261 genes and 654 in wt crush animals and 14,258 genes and 643 miRNAs in wt naive mice. mRNA was considered differentially expressed if adjusted $p$-value <0.05, whereas miRNAs were considered as such if p-value <0.05. Differentially expressed miRNA (DEMs) validated target genes were obtained using the function get_multimir from the Bioconductor/R package multiMir version 1.20.0 (Ru et al., 2014). An over-representation analysis was performed on the validated DEMs target genes and the differentially expressed genes (DEGs) by applying the enrichGO (gene ontology) function from the Bioconductor/R package clusterProfiler version 4.6.2 (Yu et al., 2012). The overrepresented GO terms with an adjusted p-value <0.05 were depicted using the emapplot or the treeplot function from the same Bioconductor/R package. Heatmaps were plotted with gplots version 3.1.3 Bioconductor/R package by using the normalized read counts, that were $Z$-score transformed. The R package ggplot2 version 3.4.1 was applied to illustrate the up- and downregulation DEMs by a volcano plot. The RNAseq and miRNAseq raw data are publicly available in the GEO repository under the following accension number GSE249877. Furthermore, to ensure that our results are not due to poor mRNA isolation quality, we included the RIN number in the supplementary material (Supplementary Table 1 S1).

### 2.5. Proteomics

For protein isolation snap frozen tissue was transferred into 150 µl (primary and secondary motor cortex, primary somatosensory cortex, striatum) and 350 µl (cerebellum) ice cold RIPA lysis buffer containing 1× protease inhibitor. The tissues were homogenized by sonification on ice (75% amplitude). Protein lysate was centrifuged at 13000 RPM for 5 min at 4 °C. Total protein concentration was determined by the Lowry assay using BSA standards. Quantitative mass spectrometry was performed by the Center for integrative and translational bioimaging, Rudolf-Virchow-Center in Wuerzburg. Similarly to Turakhiya et al. (2018), a gel electrophoresis was performed to separate the precipitated proteins. Each lane was then cut into 15 slices and further processed to extract the peptides from the gel for the NanoLC-MS/MS analysis. MaxQuant version 1.6.2.2 (Cox and Mann, 2008) was used for database search and quantification. The search was performed against the UniProt Mouse reference Proteome database, and a database containing common contaminants. Protein identification was under control of the false discovery rate (FDR; <1% FDR on protein and peptide spectrum match (PSM) level). The proteins were quantified using LFQ intensities, and only those with more than two razor/unique peptides were taken into consideration. In case of missing LFQ intensities, values were imputed using a normal distribution with a mean of the 5% quantile of the combined log10-transformed LFQ intensities and a standard deviation of 0.1. Benjamini-Hochberg adjusted $p$-values and FDR were calculated with the R package limma (Ritchie et al., 2015). The proteomic analysis detected a total of 5890 proteins in the cerebellum, 5551 proteins in the cortex and 5410 proteins in the striatum. Proteins that appeared in at least two of the replicates with a p-value <0.05 were deemed as being differentially expressed. The EnrichGO function from the Bioconductor/R package clusterProfiler version 4.6.2 was utilized to conduct an over-representation analysis. The barplot function of the same package was then employed to plot the overexpressed GO terms with an adjusted p-value <0.05. The volcanot plots were generated using the ggplot2 R package ggplot2 version 3.4.1. The proteomic raw data is publicly available in the ProteomeXchange repository under following accension number PXDO47531.

### 2.6. Statistical analysis

Every dataset was controlled for normality by the Shapiro-Wilk test using GraphPad Prism version 9.3. Nonparametric data were analyzed with the Mann-Whitney-$U$ test and Holm-Šídák multiple comparison test. Graphical representation of the data shows the mean ± standard error of mean (SEM) and statistical significance were depicted as $*p < 0.05$, $**p < 0.01$, $***p < 0.001$, $****p < 0.0001$.

### 2.7. Structural equation modelling (S.E.M.) model: construction

The S.E.M. analysis was performed using the S.E.M. toolbox for MATLAB (version 20b; Mathworks, Natick, MA, USA). S.E.M. represents a complex analytical tool that can determine the causal relationships between the variables in a model-based approach. In this model, the DEGs in the RNA between the two groups namely (DYT1KI naive vs. DYT1KI crush) from the cortex and the striatum were used as input and DEGs from the cerebellum as mediator were assessed. We explored the association with the TST data first by estimating the difference in slopes between the baseline and 12 weeks for the two groups.

### 2.8. S.E.M. model: parameter estimation

We used the Maximum Likelihood method of estimation to fit the model. To adjust the model for a longitudinal repeated measurement of the sample size, we used the Root Mean Square Error of Approximation (RMSEA) index, which improves precision without increasing bias (Kelley and Lai, 2011). The RMSEA index estimates lack of fit in a model compared to a perfect model and therefore should be low. In all models, the Invariant under a Constant Scaling (ICS) and ICS factor (ICSF) criteria should be close to zero, indicating that models were appropriate for analysis. Finally, based on the Akaike Information Criterion (AIC) the quality of each model relative to other models was estimated, with smaller values signifying a better fit of the model. The obtained criterion comparing the models varied between 0.012 and 0.038 (which indicates a good fit for the models). The strength of associations between the variables in the models was quantified by standardized coefficients (s), ranging from 0 (no association) to 1 (very strong association). The *p*-values of $<0.05$ were considered statistically significant. In addition to the AIC for the models, we have controlled the results; the adjusted Bonferroni correction severity of the adjustment was weakened with an increasing value of the average absolute correlation between two parameters in the model (Smith and Cribbie, 2013). The described significant model survived the adjusted Bonferroni correction with ($p < 0.005$).

## 3. Results

### 3.1. DYT1KI mice develop dystonia-like movements

Previous studies have demonstrated that a nerve-crush injury can induce dystonia-like features in genetically predisposed DYT-TOR1 A rodent models such as the *Tor1a*+/−, the DYT-tg mouse models and the ΔETorA rat model (Ip et al., 2016; Knorr et al., 2021; Rauschenberger et al., 2023). To test if this is also true in DYT1KI mice, we induced a nerve crush in wt and DYT1KI animals and assessed locomotion and DLM for 12 weeks after the injury (Fig. 1A). Both DYT1KI mice and wt mice developed DLM in the right hindlimb within the first two weeks following nerve crush (week 2: DYT1KI 18.14 ± 1.27 DLM/min; wt 16.65 ± 1.64 DLM/min). Wt crush mice recovered slightly from week 6 onward (week 6: 10.33 ± 1.53 DLM/min), however, they continued to show more DLM with 12.12 ± 1.66 DLM/min than wt naive mice (5.61 ± 1.04 DLM/min) even at week 12 ($p < 0.01$). In contrast, the DYT1KI crush mice showed a high level of DLM of the right hindlimb over the entire observation period, resulting in significantly more DLM/min than wt crush mice from week 6 onwards (week 6: 16.81 ± 1.32 DLM/min, $p < 0.01$; week 12: 17.18 ± 1.47 DLM/min, $p < 0.05$) (Fig. 1B). Furthermore, utilizing gait analyses, wt crush animals exhibited a reduced print width compared to their naive counterpart at week 2 (0.61 ± 0.02 cm, $p < 0.0001$), week 4 (0.68 ± 0.02 cm; $p < 0.01$) and week 6 (0.78 ± 0.02 cm, $p < 0.05$) after sciatic nerve crush. Similarly, DYT1KI crush mice displayed a smaller print width during the same time period compared to DYT1KI naive mice (week 2: 0.60 cm ± 0.03, $p < 0.0001$; week 4: 0.67 ± 0.01 cm, $p < 0.01$; week 6: 0.78 ± 0.02 cm, $p < 0.05$). By week 12, the print width of wt crush animals (0.85 ± 0.02 cm) had returned to levels comparable to wt naive animals (0.85 ± 0.02 cm). However, DYT1KI crush mice still exhibited smaller print width with 0.77 ± 0.02 cm ($p < 0.05$) at week 11 and 0.81 ± 0.02 cm ($p < 0.05$) at week 12 when compared to DYT1KI naive animals (week 11: 0.85 ± 0.02 cm; week 12: 0.89 ± 0.01 cm). All right hindlimb print width measurements are available in the supplementary material (Supplementary Table 1 S2). The stride length of animals was also investigated, considering that dystonia may induce variability in gait stride. However, no significant differences were observed among any of the group comparisons at any time point (Fig. 1D).

Taken together, these results indicate that a nerve crush injury induces more severe dystonia-like features in genetically predisposed DYT1KI mice compared to wt controls.

### 3.2. Wildtype mice develop long-lasting molecular changes in the cerebellum after sciatic nerve injury

To gain insights into the molecular changes occurring in the brain following sciatic nerve crush injury and to better understand the underlying mechanisms of overt dystonia in DYT1KI mice, we conducted a multi-omic analysis of brain tissue. Considering the significant involvement of the cerebellum in dystonia's pathophysiology, our initial focus was on this brain region. To understand the normal physiological response elicited by peripheral trauma we looked at cerebellar DEGs, DEPs, as well as the DEMs in wt crush mice compared to wt naive mice. The transcriptomic analysis revealed 1089 DEGs in the wt mice with nerve injury compared to mice without injury (Fig. 2A). GO pathway analysis revealed differential regulation in GO terms associated with transport, axogenesis, metabolic processes, translation, autophagy, regulation of catabolic processes and cell communication (Fig. 2B, supplementary Fig. S1, Supplementary Table 1 S3). These data were supported by the miRNA sequencing analysis, where 13 out of the 21 DEMs identified were linked to several of the mechanisms mentioned above, namely: metabolic processes, axogenesis, transport, autophagy, and translation (Fig. 2B & C, Supplementary Table 1 S4). This is not surprising as nearly half of the DEGs were validated target genes from the DEMs (Fig. 2D). Pathway analysis of DEPs yielded similar GO enrichments, featuring terms like mRNA processing or RNA splicing among the significant findings (Fig. 2E, supplementary Fig. S2, Supplementary Table 1 S5). Out of the 160 DEPs 10 were common with the DEGs, suggesting that some of these shared genes may play a significant role, given the presence of translation-related pathways in both datasets (Fig. 2D). Collectively, these data hint at long-lasting trauma-induced alterations in processes linked to translation in the cerebellum of wt crush mice that were visible even 12 weeks after injury.

### 3.3. DYT1KI mice fail to mount a normal translational response in the cerebellum after trauma

To test if dystonic DYT1KI mice also undergo injury-induced changes in cerebellar translation regulation, we performed the same multi-omic analysis comparing crush-injured with non-injured animals. Only 69 genes were significantly changed in the DYT1KI crush vs. DYT1KI naive animals. This modest change was in stark contrast to the 1089 genes changed in wt crush mice. Although DYT1KI animals did not mount as high a response as wt mice, ~40% of the DEGs overlapped with the DEGs of wt animals (Fig. 3A). This suggests that similar processes were initiated in both groups, although the response was not as robust in the DYT1KI animals. The relative expression of cerebellar DEGs across all groups further corroborated this theory, as the nerve injury modulated the expression of the same genes at a milder level in DYT1KI mice than in wt mice (Fig. 3B). Nerve crush injury only triggered a subtle and insignificant response to translation-related genes in DYT1KI mice (Fig. 3B). GO enrichment analysis of DEGs revealed terms encompassing the disassembly protein-containing complex, responsiveness to insulin stimuli and response to peptide (Fig. 3C, supplementary Fig. S3,

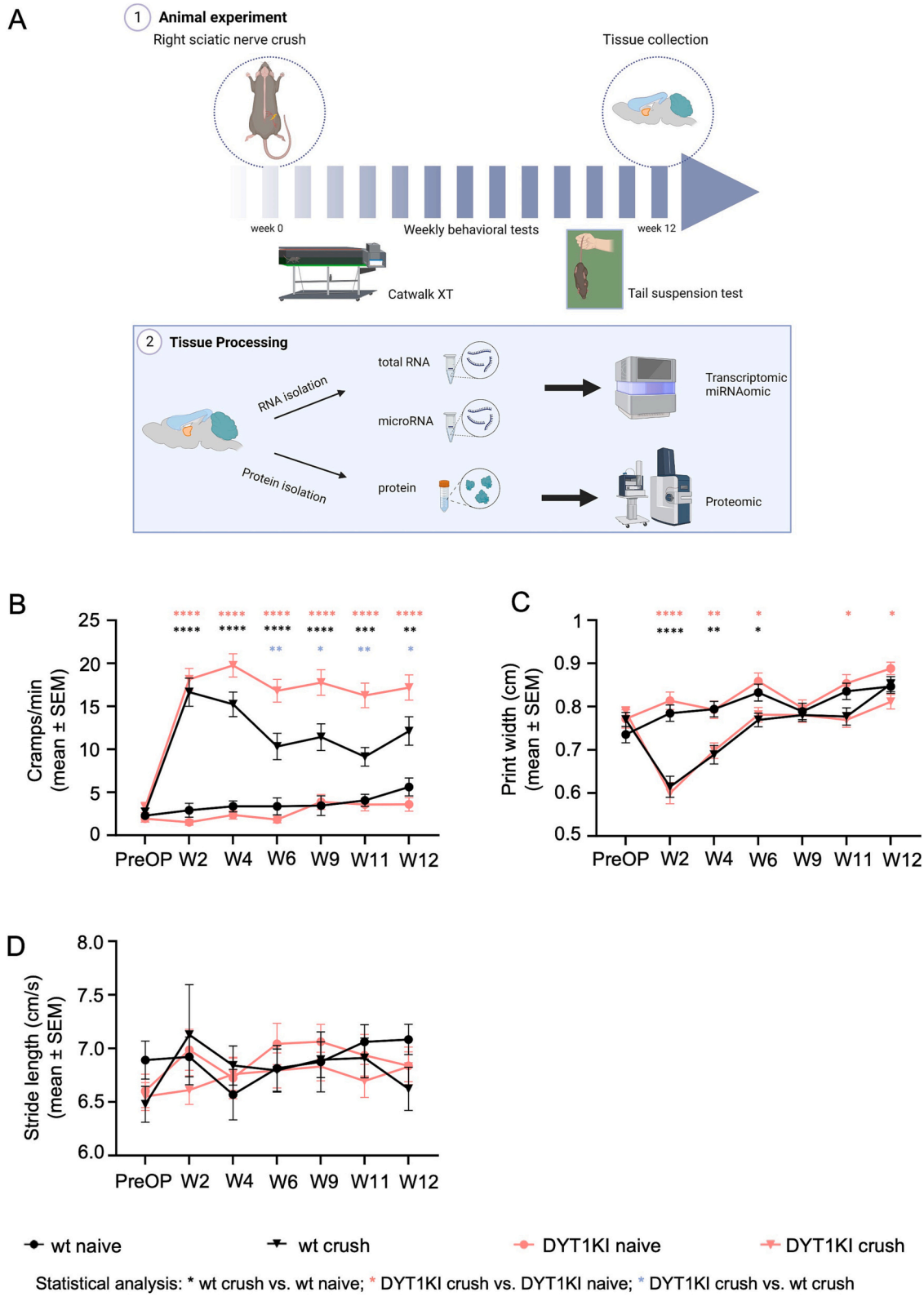


**Fig. 1.** DYT1KI mice develop DLM 12 weeks after nerve crush injury. A: Overview of the experimental design. (1) depicts the animal experiments;12 weeks old mice received a sciatic nerve crush injury and were tested at baseline and weeks 2, 4, 6, 9, 11 and 12 post surgery with the TST and Catwalk. After 12 weeks the cortex, striatum and cerebellum were collected and processed as shown in (2), before being sent for sequencing. B: Line graph depicting the TST data of wt crush ($n = 32–36$; black triangle), DYT1KI crush ($n = 45–46$; pink triangle), wt naive ($n = 30–34$; black dot) and DYT1KI naive ($n = 31–32$; pink dot) mice. C: Line graph illustrating the Catwalk data; print width in cm of wt crush ($n = 37–41$), DYT1KI crush ($n = 43–46$), wt naive (n = 30–34) and DYT1KI naive (n = 30–33) mice. D: Line graph illustrating the Catwalk data; stride length in cm/s of wt crush (n = 37–41), DYT1KI crush (n = 43–46), wt naive (n = 30–34) and DYT1KI naive (n = 30–33). All data are shown as mean ± SEM. n = number of animals. Statistical analysis for B, C Mann-Whitney test followed by Holm-Šidák multiple comparison test. Statistical analysis for D Two-way ANOVA followed by Tukey multiple comparison test. ****$p < 0.0001$, ***$p < 0.001$, **$p < 0.01$, *$p < 0.05$. A was created using Biorender. (For interpretation of the references to color in this figure legend, the reader is referred to the web version of this article.)

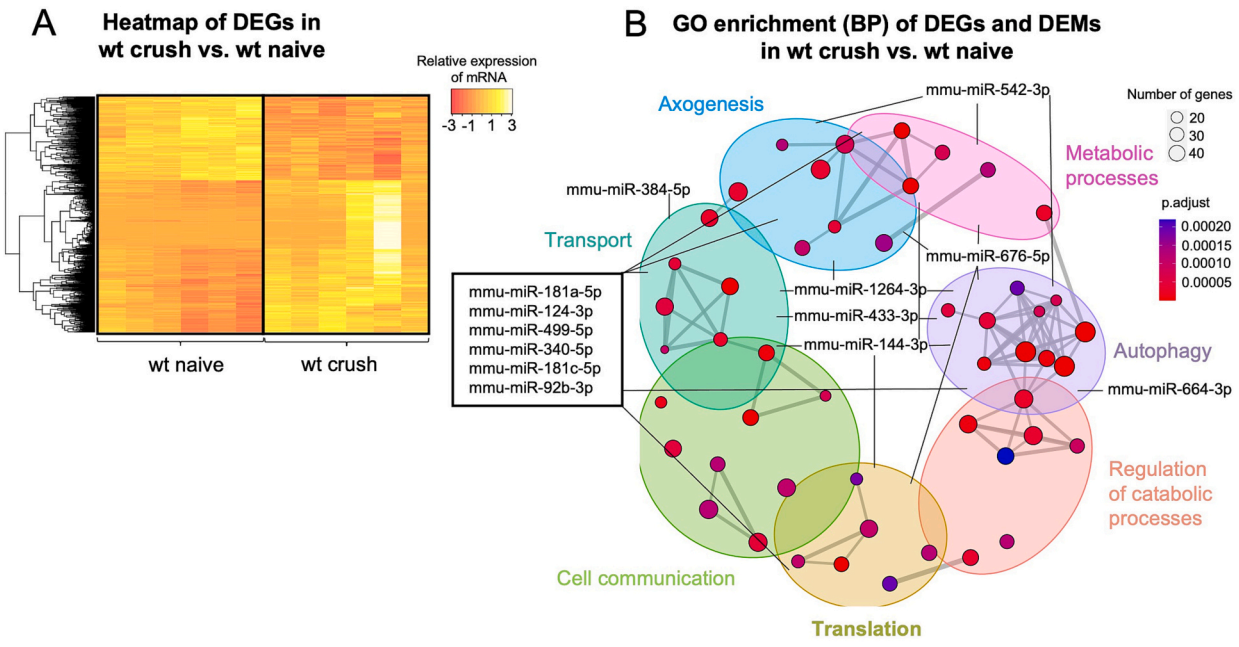


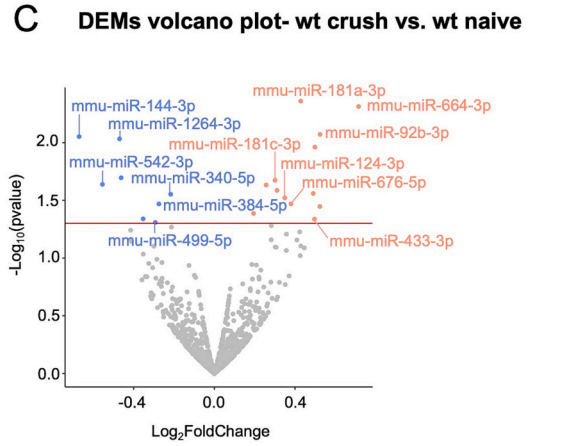


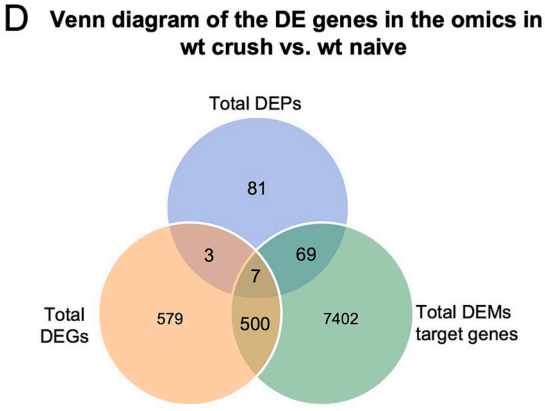


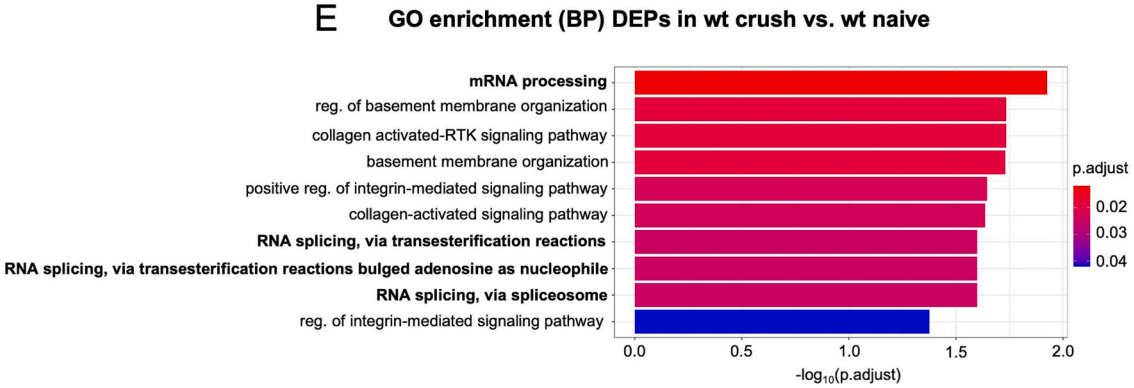


**Fig. 2.** Wt crush mice develop long-lasting molecular changes in the cerebellum. A: Heatmap of cerebellar DEGs in wt crush vs. wt naive mice. B: Emapplot of grouped GO enrichment of cerebellar DEGs and cerebellar DEMs involved in terms in wt crush vs. wt naive mice. The color of the dots represents the adjusted *p*-value, and the size stands for the number of genes involved in the GO term. C: Volcano plot of miRNAs in the cerebellum of wt crush and wt naive mice. miRNAs are color-coded, with blue representing down-regulation and red up-regulation. X-axis represents the $log_2$FoldChange, and Y represent the p-value. The red line depicts the cutoff of p-value <0.05. D: Venn diagram of all Omic data. The hypergeometric propability of shared cerebellar DEPs and DEGs is p-value <0.005, of cerebellar DEGs and DEMs target genes p-value <7.00e-112DEPs and DEMs target genes p-value <2.02e-18. E: Bar plot of cerebellar DEPs. GO enrichment in wt crush vs. wt naive mice. X-axis represents the $-log_{10}$ of adjusted p-value and colors are depicting the adjusted p-value. (For interpretation of the references to color in this figure legend, the reader is referred to the web version of this article.)

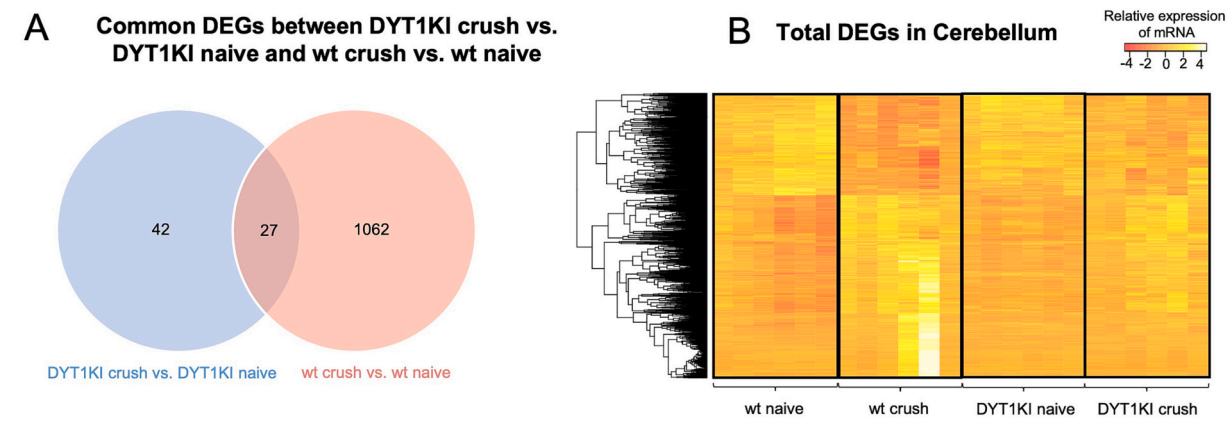


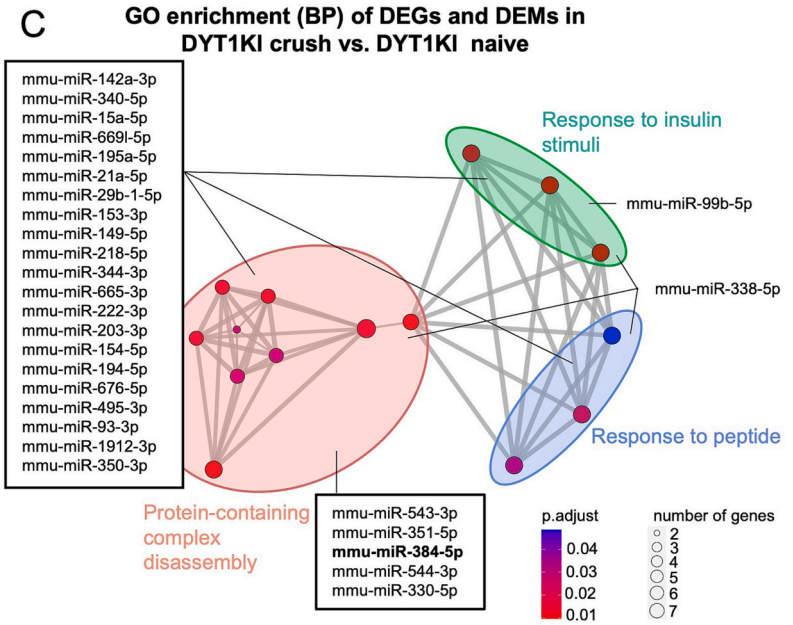


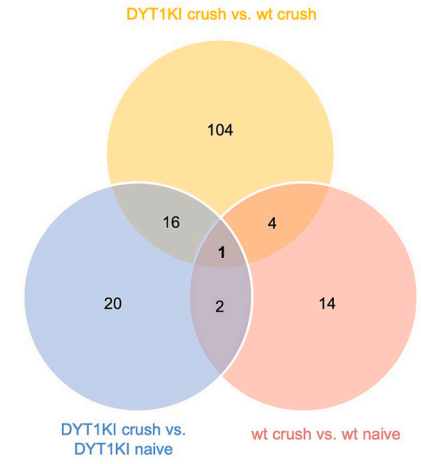


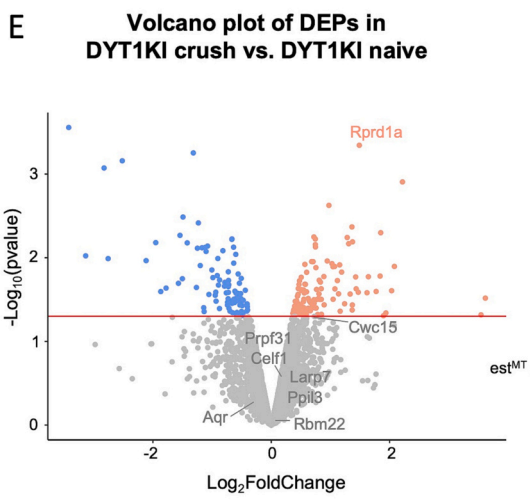


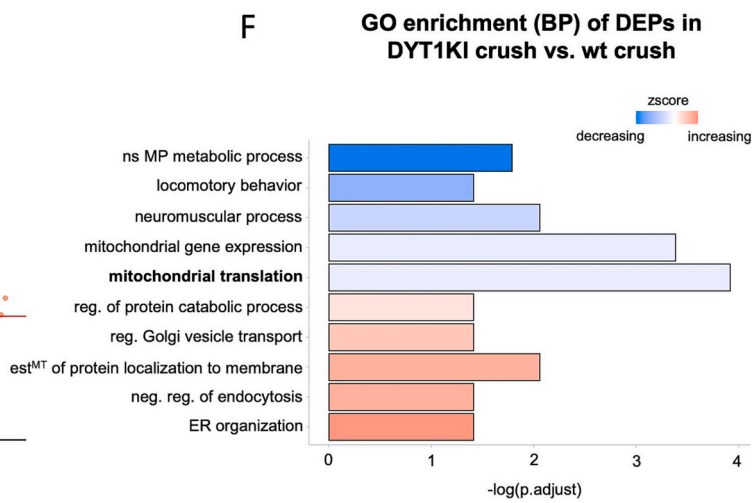


*(caption on next page)*

**Fig. 3.** DYT1KI crush mice fail to mount a normal translational response in the cerebellum. A: Venn diagram of common cerebellar DEGs between the comparison DYT1KI crush vs. DYT1KI naive and wt crush vs. wt naive animals. The hypergeometric probability of the shared cerebellar DEGs is *p*-value <2.6e-26 B: Heatmap of all DEGs in the cerebellum. C: Emapplot of grouped GO enrichment of DEGs and DEMs in the cerebellum involved in GO terms in DYT1KI crush vs. DYT1KI naive. The color of the dots represents the adjusted p-value, and the size stands for the number of genes involved in the GO term. D: Venn diagram of overlapping miRNAs in different comparisons in the cerebellum. The hypergeometric probability of shared cerebellar DEMs was calculated. The results yielded a p-value <0.008 for the DYT1KI crush vs. DYT1KI naive and wt crush vs wt naive comparison, a p-value <3.33e-11 for the DYT1KI crush vs. DYT1KI naive and DYT1KI crush vs. wt crush comparison, and a p-value <0.009 for the comparison wt crush vs. wt naive and DYT1KI crush vs. wt crush. E: Volcano plot of cerebellar DEPs in DYT1KI crush vs. DYT1KI naive. The dots are color-coded, with blue standing for downregulation, red upregulation and grey not regulated. X-axis represents the $\log_2$ fold change, and Y represent the the p-value. The red axis depicts the cutoff of p-value <0.05. F: Barplot of GO enrichment of DEPs in DYT1KI crush vs. wt crush mice. The GO terms are color-coded for their zscore with red displaying and increase and blue a decrease. The X-axis shows the –log of adjusted p-value. (For interpretation of the references to color in this figure legend, the reader is referred to the web version of this article.)

Supplementary Table 1 S6). In line with the transcriptomic data, several DEMs were involved in the GO category previously mentioned (Fig. 3C, Supplementary Table 1 S7). Three of the DEMs (mmu-miR-384-5p, mmu-miR-676-5p, mmu-miR-340-5p) were shared with the DEMs obtained from the comparison of wt crush vs wt naive. In comparison to their naive counterpart, DYT1KI crush mice exhibited a slightly higher number of DEMs, with 39 DEMs, whereas wt crush animals showed 21 DEMs. Conversely, when comparing DYT1KI crush to wt crush mice, a substantial alteration of 125 miRNAs was observed, indicating that the genotype is primarily responsible for the observed differences (Fig. 3D). Although DYT1KI crush mice exhibited significant differences in a large number of proteins (54 downregulated and 67 upregulated, Supplementary Table 1 S8), only one DEP, RPRD1A, significantly overlapped with the DEP found in wt crush animals. The remaining shared DEPs (Cwc15, Larp7, Rbm22, Prpf31, Celf1, Aqr and Ppil3) although changing similarly to wt crush mice, did not reach statistical significance (Fig. 3E). This strengthens the argument that while DYT1KI crush mice initiate similar processes as the wt crush animals, their response is diminished. Further supporting this hypothesis was the GO enrichment of DEPs in DYT1KI crush mice compared to wt crush mice, which showed a decrease in mitochondrial translation (Fig. 3F, Supplementary Table 1 S9). Altogether, the data suggest that DYT1KI crush mice fail to mount a normal translational response in the cerebellum.

### 3.4. The cortex of DYT1KI crush mice shows impairment of translational regulation

Prior studies on both manifesting and non-manifesting carrier of the torsinA mutation have demonstrated the involvement of the cortico-striatal-pallido-thalamo-cortical loop and the cerebellar-thalamo-cortical-pathway. In order to establish the potential involvement of the cortex in dystonic features development, similar multi-omic analysis were performed on cortical samples from DYT1KI crush mice. Unlike the cerebellum, a total of 1815 cortical genes were altered in DYT1KI crush vs. DYT1KI naive animals. This was in sharp contrast to the normal physiological response in wt crush animals, where only 114 genes were changed (Fig. 4A & B). These data suggest that the cortex of DYT1KI mice initiates distinct pathways following the nerve crush. Furthermore, the overlap between DYT1KI DEGs and the DEGs of wt animals was limited to approximately 4%, providing additional support for this hypothesis. Indeed, GO analysis of DYT1KI crush vs. DYT1KI naive mice revealed enrichment in translation-related mechanisms, including "mRNA processing", "ribonucleoprotein complex (RNPc) assembly", and "regulation of translation". On the other hand, wt crush vs. wt naive mice were enriched in protein degradation processes, as indicated by terms associated to the "regulation of proteasomal ubiquitin dependent protein catabolic processes" (Fig. 4C & D, Supplementary Table 1 S10, Supplementary Table 1 S11). Pathway analyses were also performed with the target genes of DEMs (Supplementary Table 1 S12). Unexpectedly, the translation-related terms displayed similar significance between the comparison wt naive vs. wt crush and DYT1KI crush vs. wt naive (Fig. 4E, Supplementary Table 1 S13). This result, which diverges from our initial expectations, could potentially be attributed to the redundancy of miRNAs (Park et al., 2010). On the other hand, the protein analysis revealed an enrichment of translation-related processes, such as "RNA localization" and "regulation of cytoplasmic translation", in DYT1KI crush animals. In contrast, to the miRNA analysis, this enrichment was specific to the DYT1KI crush animals (Fig. 4F, Supplementary Table 1 S14). Moreover, the GO pathways analysis of DEPs in DYT1KI crush vs. wt crush mice highlighted genotype-specific alterations in translation-related pathway. Specifically, the analysis revealed an increase in mitochondrial translation in DYT1KI crush mice compared to wt crush mice (Fig. 4G, Supplementary Table 1 S15). All this evidence indicates an impairment in translation regulation in the cortex of DYT1KI crush mice.

### 3.5. The striatum of DYT1KI mice with nerve injury shows impairment of translation related processes

As previously mentioned, dystonia has been associated with the involvement of the cortico-striatal-pallido-thalamo-cortical pathway (Niethammer et al., 2011). Therefore, we conducted the same omics analysis for the striatum as we did for the cerebellum and cortex. In the striatum, DYT1KI crush animals exhibited a significantly higher number of DEGs (545 DEGs) compared to wt crush animals (4 DEGs) when compared to their respective naive counterpart. This mirrors the finding in the cortex, indicating the activation of distinct pathways in the DYT1KI striatum (Fig. 5A). The ensuing GO enrichment analysis demonstrated various processes related to translation, including "mRNA processing", "regulation of translation" or "cytoplasmic translation" (Fig. 5B, Supplementary Table 1 S16). Once again, those findings were consistent with the ones obtained in the cortex. Furthermore, a number of these translation-related processes were also enriched in the miRNA analysis, including: "regulation of translation", "regulation of mRNA metabolic processes" and "mRNA processing" (Fig. 5C, Supplementary Table 1 S17). The study of the DEPs further supported the involvement of translation-related processes in DYT1KI crush animals, as enrichment analysis revealed terms such as: "RNPc assembly", "cytoplasmic translation" or "ribosome assembly" (Fig. 5D, Supplementary Table 1 S18, Supplementary Table 1 S19). In contrast, DEPs in wt crush mice were only significantly enriched in: "Rab protein signal transduction", "Ras protein signal transduction" and "adherens junction organization" (Supplementary Table 1 S20). The genotype specificity of our findings was underscored by the analysis of DEPs in DYT1KI crush vs. wt crush mice, revealing increased activity in cytoplasmic translation (Fig. 5E, Supplementary Table 1 S21).These results hint towards a dysregulation in the processes related to translation in both the cortex and the striatum of DYT1KI mice following a sciatic nerve injury. It is conceivable that these dysregulations are intricately linked to the development of the observed DLM in these animals.

### 3.6. The S.E.M. model predicts difference between DYT1KI crush and DYT1KI naive behavior slope by using RNAseq data

The obtained fit indices for the model in the structural equation modelling analysis implied a good fit for the constructed model to the observed data, providing robust causal relations between the variables. In the model the input of DEGs in the cortex together with the striatum

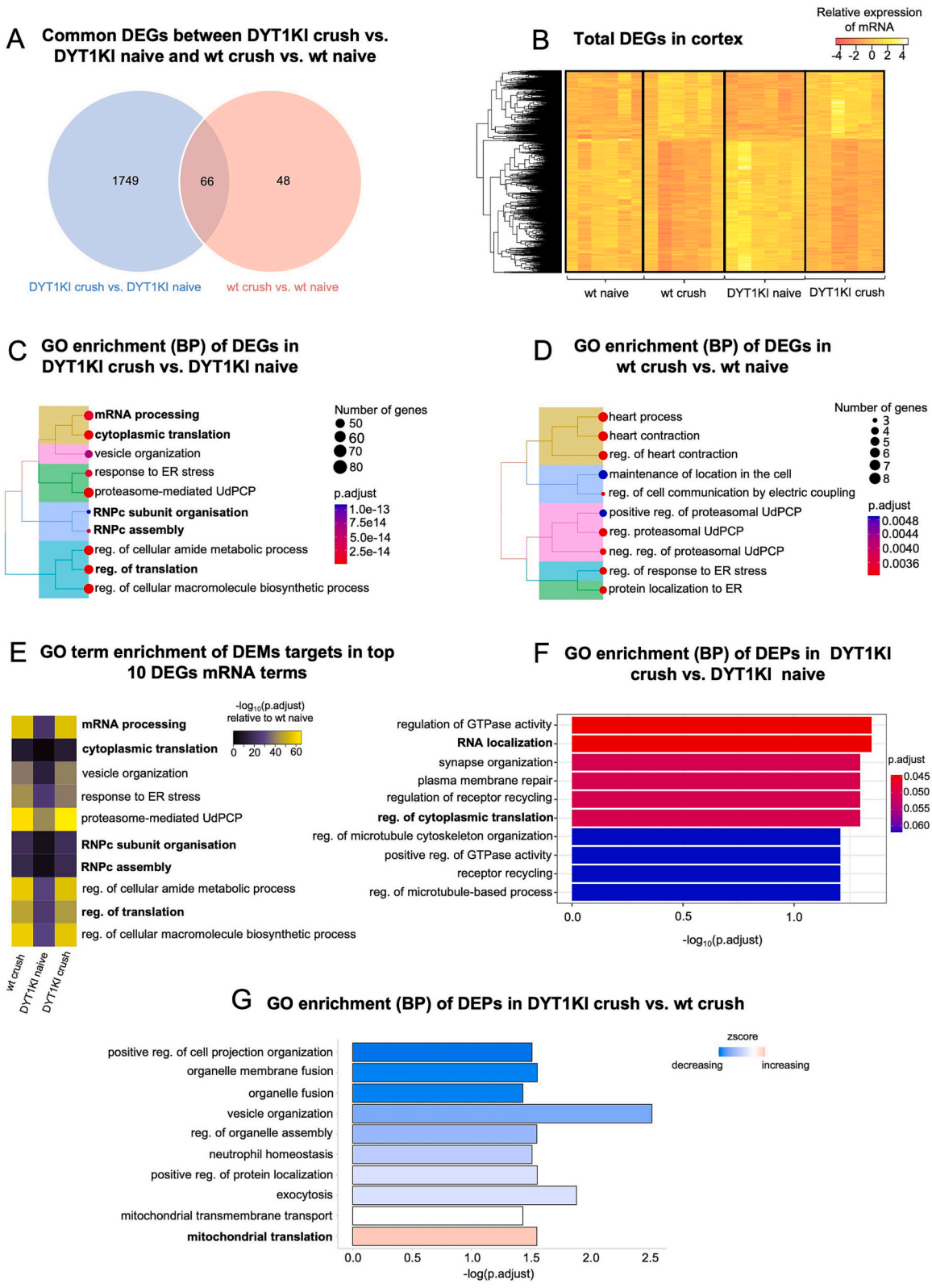


**Fig. 4.** Cortex of DYT1KI crush mice shows impairment in translational related processes. A: Venn diagram of the cortical DEGs in the comparison DYT1KI crush vs. DYT1KI naive and wt crush vs. wt naive. The hypergeometric probability of the shared cortical DEGs is *p*-value <6.18e-62. B: Heatmap of all DEGs in cortex. C: Treeplot depicting the pathways of the cortical DEGs enrichment analysis in DYT1KI crush vs. DYT1KI naive. The dots color represents the adjusted p-value and the size the number of genes involved in the term. D: Treeplot depicting GO pathways of the cortical DEGs enrichment analysis in wt crush vs. wt naive. The dots color represents the adjusted p-value and the size the number of genes involved in the term. E: Heatmap of the GO term enrichment of cortical DEMs targets in DEGs GO term. The map is color coded by $-\log_{10}$ of the adjusted p-value relative to wt naive animals. F: Barplot of GO term of the cortical DEPs in DYT1KI crush vs. DYT1KI naive mice. X-axis represents the $-\log_{10}$ of adjusted p-value and colors are depicting the adjusted p-value. G: Barplot of the enriched GO terms in the cortical DEPs of DYT1KI crush vs. wt crush mice. The bars are color-coded for the zscore of the pathways with red indicating and increase and blue a decrease. The X-axis represents the – log of adjusted p-value. (For interpretation of the references to color in this figure legend, the reader is referred to the web version of this article.)

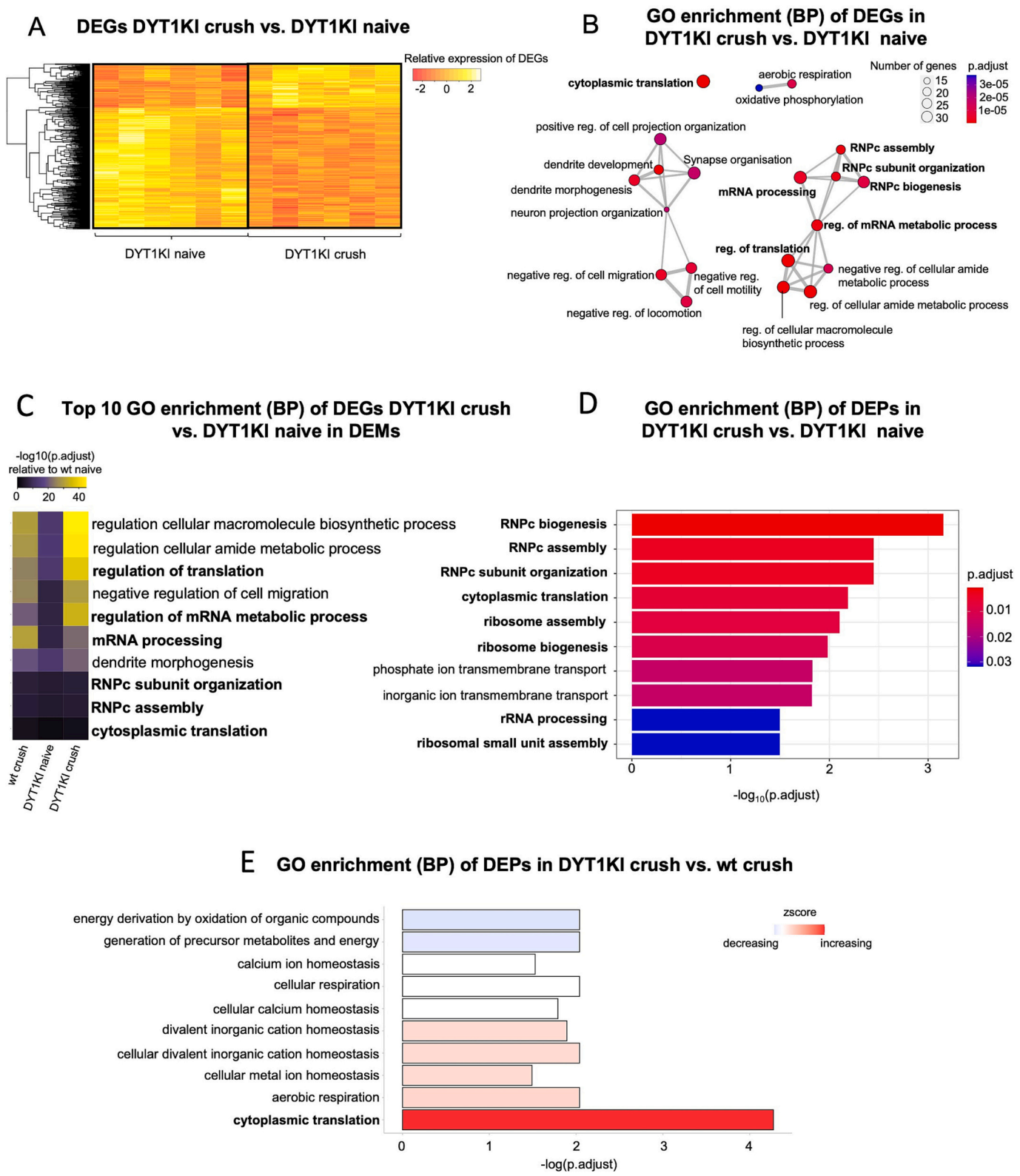


**Fig. 5.** Striatum of DYT1KI crush mice show impairment in translational related processes. A: Heatmap of striatal DEGs in DYT1KI crush vs. DYT1KI naive. B: Emapplot of striatal DEGs enrichment analysis in DYT1KI crush vs. DYT1KI naive. Dots size represent the numbers of genes in GO term and color represent the adjusted *p*-value. C: Heatmap of the GO term enrichment of striatal DEMs targets in DEGs GO term. The map is color coded by $-\log_{10}$ of the adjusted p-value relative to wt naive animal. D: Barplot of GO term of the striatal DEPs in DYT1KI crush vs. DYT1KI naive mice. X-axis represents the $-\log_{10}$ of adjusted p-value and colors are depicting the adjusted p-value. E: Barplot of GO enrichment of striatal DEPs in DYT1KI crush vs. wt crush animals. The colors of the map represent the zscore of the GO terms, with red indicating an increase and blue a decrease. The X-axis stands for the –log of adjusted p-value. (For interpretation of the references to color in this figure legend, the reader is referred to the web version of this article.)

and same parameters from the cerebellum as mediator were strong predictors for the behavior slopes (standardized coefficient S = 0.74; $p < 0.01$) as shown in Fig. 6. In addition, from this model we did not find direct significant predictors for the DEGs in the cerebellum using the DEGs in the cortex (S = 0.25; $p > 0.05$) or with the DEGs in the striatum (S = 0.36; p > 0.05). Various combinations of inputs DEGs from different brain regions in the S.E.M. model were explored. However, these models failed to predict the behavioral slope (supplementary Fig. 4). The current prediction model provides additional support for our transcriptomic findings, suggesting that dysregulations in all three brain regions are required for the development of a dystonic phenotype in genetically predisposed individuals.

## 4. Discussion

Literature has long reported dystonia patients whose onset of symptoms occurred in relation to an injury. While sciatic nerve lesions themselves have not been identified to cause dystonic movement, both head and peripheral trauma have been described as risk factors associated with dystonia (Defazio et al., 1998; Frei et al., 2004; Jankovic and Van der Linden, 1988; Macerollo et al., 2019). Peripheral nerve crush injuries happen when the nerve is compressed, without complete transection, enabling the regeneration of the nerve (Menorca et al., 2013). Nevertheless, the denervation induces alteration in the central network of the brain that persist even after regeneration (Humanes-Valera et al., 2014; Ueta and Miyata, 2021). These findings hint towards the involvement of extragenetic factors in the development of dystonia. The presence of symptomatic and asymptomatic DYT-TOR1A mutation carriers further supports this "second hit hypothesis", postulating that a genetic and environmental trigger is needed to develop a clinical phenotype. Here, we were able to replicate results from previous work on different DYT-TOR1A rodent models, using a sciatic nerve crush to elicit DLM in DYT1KI mice. Independent of the genotype, crush animals displayed clenching and retraction of the hind paw starting two weeks after sciatic crush injury. These movements were considered as "pseudodystonia", mostly due to proprioceptive and sensory loss caused by the injury (Berlot et al., 2019). Nevertheless, it is noteworthy that around 8 weeks after surgery, the nerve is presumed to have substantially regained its functional capacities (Bridge et al., 1994). Electroneurography measurements performed 10 weeks following the nerve crush injury, showed no main effect of genotype, suggesting that the recovery is not different between DYT1KI and wt mice (supplementary Fig. S5). The equal recovery rate in both genotypes in combination with a higher rate of DLM in the DYT1KI crush mice compared to wt mice, points towards maladaptive processes in the genetically-predisposed animals. While wt crush animals remain affected even in week 12, DYT1KI crush mice present significantly more DLM in comparison. Similarly, both wt and DYT1KI crush animals had smaller print width of the ipsilateral paw during the first weeks after surgery. This is in line with data from Bozkurt et al., 2008, which showed a reduction of print length and print width, among others, after a sciatic nerve injury in rats. Over the course of the 12 weeks experiment, the animals recovered to nearly preoperative value starting at week 7 (Bozkurt et al., 2008). We can therefore assume that the smaller print width we observed in the first weeks after nerve crush are due to the surgical intervention. In contrast, the differences discovered after week 6 in our experiments may be associated with the development of a dystonic phenotype following a sciatic nerve crush injury. This dystonic phenotype can lead to central motor network changes, resulting in cramping of the hind paw and thus higher DLM. The smaller width observed in the right hindlimb paw of DYT1KI mice may be a consequence of increased cramping following peripheral nerve injury. The phenotypical motor abnormalities resulting from the peripheral nerve lesion may be due to central network changes. To examine molecular changes in DYT1KI and control mice, we used an unbiased multi-omics approach. In our study, we observed translation-associated processes at various molecular levels in the cerebellum of wt crush mice but not DYT1KI crush mice. Over the years, studies have demonstrated a crucial role of cerebellum in the development of dystonia. For instance, in tottering mice, a cerebellectomy was able to reduce and even eliminate dystonic attacks (Neychev et al., 2008). On the other hand, in wt mice, injecting an excitatory glutamate receptor agonist (kainic acid) into the cerebellum resulted in the manifestation of dystonic phenotype (Alvarez-Fischer et al., 2012; Pizoli et al., 2002). Prior studies have demonstrated a link between translational mechanisms and synaptic plasticity. To modulate the synaptic strength through short- or long-lasting changes, new protein synthesis is required and enabled through local translation (Kelleher 3rd et al., 2004; Klann et al., 2004). Based on our data analysis, we found that the proteins enriched in translation-related processes in the wt crush vs. wt naive comparison were unchanged in the DYT1KI crush animals. Additionally, the analysis of cerebellar proteins in DYT1KI crush mice revealed a decrease in activity in mitochondrial translation when compared to wt crush mice. Similarly, the miRNAs did not significantly differ betweenthe two comparisons, wt crush vs. wt naive and DYT1KI crush vs DYT1KI naive. This is in line with one of the common characteristics of dystonia pathophysiology, known as maladaptive synaptic plasticity (Balint et al., 2018; Quartarone and Hallett, 2013). In accordance with this, Purkinje cells in DYT1KI mice have fewer and thinner dendrites with fewer spines, indicating abnormal cerebellar signaling (Song et al., 2014). Cerebellar proteins were also enriched in terms associated with the basement membrane, collagen and integrins in wt crush mice. These components interact with each other and have been linked to synaptic plasticity. Altered synaptic plasticity has been observed in diverse integrin knock-out hippocampal neurons (Chan et al., 2006; Cingolani

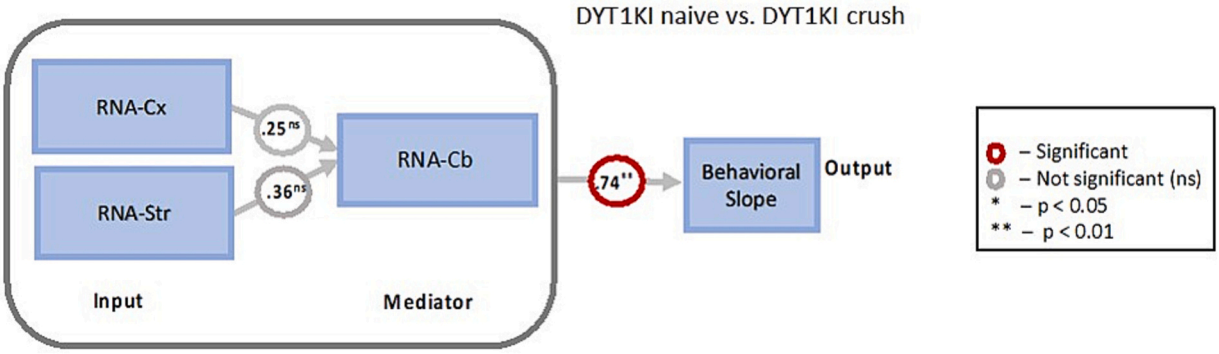


**Fig. 6.** RNA sequencing of DYT1KI brain tissue predicts behavioral deficits in dystonic mice. Structural equation modelling demonstrates that DEGs in cortex and striatum (as input) and DEGs in the cerebellum (as mediator) were able to predict the difference in behavioral slope between the DYT1KI naive and DYT1KI crush mice. Standardized coefficients significant at $p < 0.01$ are shown in red. The non-significant values are shown in grey $p > 0.05$. (For interpretation of the references to color in this figure legend, the reader is referred to the web version of this article.)

and Goda, 2008). Additionally, the extracellular matrix (ECM), in which collagen is a major component, plays a role in the functional synaptic complex. The absence of ECM components has been reported to impact synaptic plasticity (Frischknecht and Gundelfinger, 2012). In the case of Purkinje cells, it was shown that a weakened inhibitory input under certain conditions resulted in a reduction in the thickness of the perineuronal nets, a specialized ECM. Conversely, if those inputs are strengthened, the thickness of the perineuronal nets increases (Foscarin et al., 2011). The presence of basement membrane, collagen and integrin terms in the analysis supports the notion that cerebellar synaptic plasticity may play a role in preventing or reducing DLM in wt animals. The translation-associated pathways discovered in the wt crush mice are likely a rescue mechanism that is absent in the DYT1KI crush mice. Interestingly, translation-related pathways were also enriched in cerebellar DEPs of DYT1KI naive mice when compared to wt naive mice (supplementary Fig. S6). This finding further supports the hypothesis of a rescue mechanism in the cerebellum associated with translational pathways. The absence of these pathways in the cerebellum may explain why DYT1KI crush mice exhibit higher DLM compared to wt crush and DYT1KI naive mice. Proteomic analysis of DYT-TOR1A rodent models' brain is scarce. So far, only cerebellar proteins in an induced ER-stress DYT1KI mouse model have shown a disruption in the ER protein processing pathway and in calcium dynamics (Beauvais et al., 2016). In contrast, our data revealed no significant GO enrichment of the DEPs in DYT1KI crush mice. One possible explanation for this disparity might be the age at which the proteome analysis was performed. Cerebellar torsinA levels are the highest during the postnatal day 7 to day 14 before gradually decreasing (Vasudevan et al., 2006). The prior study investigated the proteome of three-week-old mice, whereas our study focused on 6 months old mice. As a result, it is probable that the changes observed are due to the higher amount of mutated torsinA found in three-week-old mice. Furthermore, the stressor chosen might be of consequence. In this study, we opted for a one-time mechanical stressor, from which the animal could recover, as opposed to an intrinsic one.

In contrast to our observation in cerebellar tissue, DEGs, DEPs, and DEMs in striatal and cortical tissue of DYT1KI mice were enriched in pathways related to translation and also in the biogenesis of ribonucleoprotein (RNP) complex. RNP transports specific mRNAs to different cellular areas, where the mRNA can be locally translated (Richter, 2001). This event has been demonstrated in neurons, where specific mRNAs are transported to the axons or dendrites for local translation (Thelen and Kye, 2019). A study in drosophila showed that changes in Torsin function led to the sequestration of megaRNP at the nuclear envelope. This occurred due to the absence of scission at the inner nuclear membrane, resulting in altered transcript localization in the nucleus and at synaptic site, causing a decreased protein synthesis (Jokhi et al., 2013). The accumulation of RNP at the nuclear envelope appears similar to a phenomenon observed in neuronal cells, where cells carrying the DYT-TOR1A mutation displayed abnormal vesicle structure at the nuclear envelope (Gonzalez-Alegre and Paulson, 2004; Hewett et al., 2000). Moreover, enrichment of DEPs in DYT1KI mouse embryonic fibroblast (MEF) showed a dysregulation in RNP export when exposed to cellular stress (Shroff et al., 2021). In contrast, the GO pathway analysis of striatal DEPs in DYT1KI naive mice vs. wt naive mice included terms linked to transport such as "protein localization to cell periphery", or "protein localization to plasma membrane". Additionally, other GO terms demonstrated enrichment in processes such as "organelle fusion", "vesicle fusion" and "membrane fusion" (supplementary Fig. S7). Together, these results could support the proposed concept by Jokhi et al., 2013, which suggests that the ΔGAG mutation in TorsinA leads to neuropathological abnormalities, including dysregulation in synaptic plasticity. Other RNA studies of DYT-TOR1A rodent model's striatum demonstrated an enrichment in the sprouting of corticospinal neurons, projection of motor and sensory axons, excitation of the postsynaptic region, dysregulation of eIF2α signaling, mitochondrial dysfunction and protein ubiquitination, among others (Beauvais et al., 2018; Grundmann et al., 2008; Mitchell et al., 2019). This is consistent with our transcriptomic results that identified enrichment in oxidative phosphorylation, dendrite development and neuron projection organization and others. Studies on DYT-TOR1A carriers manifesting dystonia have reported enlarged dopaminergic cell bodies in the substantia nigra compared to non-manifesting DYT-TOR1A carriers (Iacono et al., 2019). Similar results have been observed in the DYT1KI mouse model (Song et al., 2014). Additionally, abnormalities in dopamine signaling and a reduction in striatal dopamine receptors (DR2, DR1) at the protein level have been reported, despite unchanged mRNA levels(Dang et al., 2012; Yokoi et al., 2015). In other DYT-TOR1A models, such as the *Tor1a*+/− mouse model, mixed results have been described. Bonsi et al., 2019 observed decreased striatal dopamine receptors (D2R andD1R) only at the protein level, whereas Ip et al., 2016 found a reduction at both the protein and mRNA level using the same mouse model. Furthermore, alterations in the cholinergic system have been observed. A mouse model with a specific knockout of ΔGAG torsinA in cholinergic interneurons exhibited lower numbers of striatal cholinergic interneurons. This was accompanied by a reduction in striatal choline acetyltransferase protein levels (Liu et al., 2021). In the *Tor1a*+/− mouse model, the protein levels of vesicular acetylcholine transporter were increased, while the mRNA levels were not (Tassone et al., 2021).

Surprisingly, we did not find any changes associated with those mechanisms. It is possible that the aberrancies in whole striatum lysate were too small and below the detection level in our mouse model. Single cell sequencing of medium spiny neurons might offer a better insight into the role of the dopaminergic system in DYT-TOR1A dystonia. Neuroanatomical and imaging studies in human and mice over the years have implicated the cortex in dystonia. However, only few studies have looked at the molecular changes in the cortex. In our study, we discovered significant translational and RNP-related changes, hinting towards a potential dysregulation of cortical synaptic plasticity in DYT1KI crush mice. Additionally, the pathway analysis of cortical DEPs in DYT1KI naive vs. wt naive mice also unveiled GO terms related to "cytoplasmic translation", as well as several processes associated with transport and energy metabolism (supplementary Fig. S8). These observations imply the presence of a predisposing endophenotype in DYT1KI mice on protein-level that shifts primarily towards regulation of cytoplasmic translation and calcium homeostasis following sciatic nerve crush injury. Our data adds to the already existing electrophysiological evidence, showing abnormal inhibitory circuits in the cortex, disrupting the homeostatic plasticity (Quartarone et al., 2003; Quartarone and Hallett, 2013). Maladaptive plasticity can also be found at the corticostriatal synapse, as shown by the loss of long-term depression in a mouse model overexpressing the human mutated TorsinA (Martella et al., 2009). It was thus little surprising to find similar affected pathways in cortex and the striatum. Since dystonia is known to be a motor network disorder, it is tempting to think that our data show an issue in communication between the studied brain areas. The possible lack of localized translation caused by of the RNP's inability to export from the nucleus, may contribute to the loss of homeostatic plasticity at the corticostriatal synapse, as well as synapses involved in the cerebello-thalamico-cortico circuit. In dystonic tremor syndrome, the tremor activity was mostly localized in the cerebellum and the thalamic-cerebello connectivity was altered (Nieuwhof et al., 2022). Based on this, we hypothesized that the DYT1KI crush animals displayed more DLM due to the abnormal plasticity in the cortex and the striatum. Moreover, the inability to regulate translation-related pathways in the cerebellum could also contribute to the observed motor abnormalities.

Taking advantage of the multi-regional RNA sequencing dataset obtained from our dystonia mice, we employed structural equation modelling to identify whether our RNA sequencing data could be used to predict DLM comparing DYT1KI mice with and without nerve crush injury. Intriguingly, combining all three brain regions (cortex, striatum and cerebellum) could predict DLM in DYT1KI mice.

To conclude, our study has provided evidence that an extragenetic

factor can lead to DLM in genetically predisposed DYT-TOR1A mice. This unbiased descriptive study showed reduced capacity of compensatory translational mechanisms in the cerebellum of DYT1KI crush mice. In addition, cortical and striatal translation dysregulations seem to be necessary to cause a dystonic phenotype in DYT1KI crush mice. These findings highlight the interplay between genetic predisposition and environmental factors, contributing to the understanding of dystonia pathophysiology.

Supplementary data to this article can be found online at https://doi.org/10.1016/j.nbd.2024.106453.

## Funding

This project was funded by the European Union's Horizon 2020 Research and Innovation Programme under the EJP RD COFUND-EJP N° 825575 (EurDyscover) and by the VERUM Foundation. Moreover, C.W.I., J.V. and M.S. receive funding from the Deutsche Forschungsgemeinschaft (DFG, German Research Foundation) Project-ID 424778381-TRR 295 (A01, A05, A06) and the Interdisciplinary Center for Clinical Research (IZKF) at the University of Würzburg (S-506, N-362). In addition, L.R. receives funding from the Interdisciplinary Center for Clinical Research (IZKF) at the University of Würzburg (ZZ-29) and from the Dystonia Medical Research Foundation (Postdoctoral Research Fellowship).

## Authors' contributions

C.W.I., C.R., S.K. designed the experiments. C.R., S.K. performed the experiments. R.L.M., L.R., M.M. P. A., T.G., A.S. analyzed the data. C.R., S.K. and L.R. wrote the manuscript. C.R. designed the figs. C.W.I., M.S. and J.V. reviewed and edited the manuscript. All authors read and approved the final manuscript.

## Acknowledgements

We thank Veronika Senger and Stephanie Lamer for their technical support.

## CRediT authorship contribution statement

**Colette Reinhold:** Writing – original draft, Investigation, Formal analysis. **Susanne Knorr:** Writing – original draft, Supervision, Methodology, Investigation, Formal analysis. **Rhonda L. McFleder:** Investigation, Formal analysis. **Lisa Rauschenberger:** Writing – original draft, Software, Investigation. **Muthuraman Muthuraman:** Writing – original draft, Methodology, Investigation. **Panagiota Arampatzi:** Methodology, Investigation. **Tom Gräfenhan:** Methodology, Investigation. **Andreas Schlosser:** Methodology, Investigation. **Michael Sendtner:** Writing – review & editing, Validation, Methodology. **Jens Volkmann:** Writing – review & editing, Validation, Funding acquisition. **Chi Wang Ip:** Writing – review & editing, Validation, Supervision, Resources, Project administration, Funding acquisition, Conceptualization.

## Declaration of competing interest

The authors report no conflicts of interest.

## Data availability

The RNA and miRNA sequencing datasets generated and analyzed during the current study are available at GEO (http://www.ncbi.nlm.nih.gov/geo) under the accession number GSE249877. The mass spectrometry proteomics data have been deposited to the ProteomeXchange Consortium via the PRIDE partner repository with the dataset identifier PXD047531.

## References

Albanese, A., Bhatia, K., Bressman, S.B., Delong, M.R., Fahn, S., Fung, V.S., Hallett, M., Jankovic, J., Jinnah, H.A., Klein, C., Lang, A.E., Mink, J.W., Teller, J.K., 2013. Phenomenology and classification of dystonia: a consensus update. Mov. Disord. 28 (7), 863–873. https://doi.org/10.1002/mds.25475.

Alvarez-Fischer, D., Grundmann, M., Lu, L., Samans, B., Fritsch, B., Moller, J.C., Schaefer, M.K., Hartmann, A., Oertel, W.H., Bandmann, O., 2012. Prolonged generalized dystonia after chronic cerebellar application of kainic acid. Brain Res. 1464, 82–88. https://doi.org/10.1016/j.brainres.2012.05.007.

Balint, B., Mencacci, N.E., Valente, E.M., Pisani, A., Rothwell, J., Jankovic, J., Vidailhet, M., Bhatia, K.P., 2018. Dystonia. Nat. Rev. Dis. Primers 4 (1), 25. https://doi.org/10.1038/s41572-018-0023-6.

Beauvais, G., Bode, N.M., Watson, J.L., Wen, H., Glenn, K.A., Kawano, H., Harata, N.C., Ehrlich, M.E., Gonzalez-Alegre, P., 2016. Disruption of protein processing in the endoplasmic reticulum of DYT1 Knock-in mice implicates novel pathways in dystonia pathogenesis. J. Neurosci. 36 (40), 10245–10256. https://doi.org/10.1523/JNEUROSCI.0669-16.2016.

Beauvais, G., Rodriguez-Losada, N., Ying, L., Zakirova, Z., Watson, J.L., Readhead, B., Gadue, P., French, D.L., Ehrlich, M.E., Gonzalez-Alegre, P., 2018. Exploring the interaction between eIF2alpha dysregulation, acute endoplasmic reticulum stress and DYT1 dystonia in the mammalian brain. Neuroscience 371, 455–468. https://doi.org/10.1016/j.neuroscience.2017.12.033.

Berlot, R., Bhatia, K.P., Kojovic, M., 2019. Pseudodystonia: a new perspective on an old phenomenon. Parkinsonism Relat. Disord. 62, 44–50. https://doi.org/10.1016/j.parkreldis.2019.02.008.

Bonsi, P., Ponterio, G., Vanni, V., Tassone, A., Sciamanna, G., Migliarini, S., Martella, G., Meringolo, M., Dehay, B., Doudnikoff, E., Zachariou, V., Goodchild, R.E., Mercuri, N. B., D'Amelio, M., Pasqualetti, M., Bezard, E., Pisani, A., 2019. RGS9-2 rescues dopamine D2 receptor levels and signaling in DYT1 dystonia mouse models. EMBO Mol. Med. 11 (1) https://doi.org/10.15252/emmm.201809283.

Bozkurt, A., Deumens, R., Scheffel, J., O'Dey, D.M., Weis, J., Joosten, E.A., Fuhrmann, T., Brook, G.A., Pallua, N., 2008. CatWalk gait analysis in assessment of functional recovery after sciatic nerve injury. J. Neurosci. Methods 173 (1), 91–98. https://doi.org/10.1016/j.jneumeth.2008.05.020.

Bridge, P.M., Ball, D.J., Mackinnon, S.E., Nakao, Y., Brandt, K., Hunter, D.A., Hertl, C., 1994. Nerve crush injuries–a model for axonotmesis. Exp. Neurol. 127 (2), 284–290. https://doi.org/10.1006/exnr.1994.1104.

Carbon, M., Argyelan, M., Ghilardi, M.F., Mattis, P., Dhawan, V., Bressman, S., Eidelberg, D., 2011. Impaired sequence learning in dystonia mutation carriers: a genotypic effect. Brain 134 (Pt 5), 1416–1427. https://doi.org/10.1093/brain/awr060.

Chan, C.S., Weeber, E.J., Zong, L., Fuchs, E., Sweatt, J.D., Davis, R.L., 2006. Beta 1-integrins are required for hippocampal AMPA receptor-dependent synaptic transmission, synaptic plasticity, and working memory. J. Neurosci. 26 (1), 223–232. https://doi.org/10.1523/JNEUROSCI.4110-05.2006.

Cingolani, L.A., Goda, Y., 2008. Differential involvement of beta3 integrin in pre- and postsynaptic forms of adaptation to chronic activity deprivation. Neuron Glia Biol. 4 (3), 179–187. https://doi.org/10.1017/S1740925X0999024X.

Cox, J., Mann, M., 2008. MaxQuant enables high peptide identification rates, individualized p.p.b.-range mass accuracies and proteome-wide protein quantification. Nat. Biotechnol. 26 (12), 1367–1372. https://doi.org/10.1038/nbt.1511.

Dang, M.T., Yokoi, F., Cheetham, C.C., Lu, J., Vo, V., Lovinger, D.M., Li, Y., 2012. An anticholinergic reverses motor control and corticostriatal LTD deficits in Dyt1 DeltaGAG knock-in mice. Behav. Brain Res. 226 (2), 465–472. https://doi.org/10.1016/j.bbr.2011.10.002.

Defazio, G., Berardelli, A., Abbruzzese, G., Lepore, V., Coviello, V., Acquistapace, D., Capus, L., Carella, F., De Berardinis, M.T., Galardi, G., Girlanda, P., Maurri, S., Albanese, A., Bertolasi, L., Liguori, R., Rossi, A., Santoro, L., Tognoni, G., Livrea, P., 1998. Possible risk factors for primary adult onset dystonia: a case-control investigation by the Italian movement disorders study group. J. Neurol. Neurosurg. Psychiatry 64 (1), 25–32. https://doi.org/10.1136/jnnp.64.1.25.

Draganski, B., Schneider, S.A., Fiorio, M., Kloppel, S., Gambarin, M., Tinazzi, M., Ashburner, J., Bhatia, K.P., Frackowiak, R.S., 2009. Genotype-phenotype interactions in primary dystonias revealed by differential changes in brain structure. Neuroimage 47 (4), 1141–1147. https://doi.org/10.1016/j.neuroimage.2009.03.057.

Edwards, M.J., Huang, Y.Z., Mir, P., Rothwell, J.C., Bhatia, K.P., 2006. Abnormalities in motor cortical plasticity differentiate manifesting and nonmanifesting DYT1 carriers. Mov. Disord. 21 (12), 2181–2186. https://doi.org/10.1002/mds.21160.

Foscarin, S., Ponchione, D., Pajaj, E., Leto, K., Gawlak, M., Wilczynski, G.M., Rossi, F., Carulli, D., 2011. Experience-dependent plasticity and modulation of growth regulatory molecules at central synapses. PLoS One 6 (1), e16666. https://doi.org/10.1371/journal.pone.0016666.

Frei, K.P., Pathak, M., Jenkins, S., Truong, D.D., 2004. Natural history of posttraumatic cervical dystonia. Mov. Disord. 19 (12), 1492–1498. https://doi.org/10.1002/mds.20239.

Frischknecht, R., Gundelfinger, E.D., 2012. The brain's extracellular matrix and its role in synaptic plasticity. Adv. Exp. Med. Biol. 970, 153–171. https://doi.org/10.1007/978-3-7091-0932-8_7.

Gelisin, O., Susgun, S., Toruntay, C., Yabaci, A., Baran, G., Gursoy, A.E.B., Yildiz, G.B., Yucesan, E., 2023. Evaluation of miR-526b-3p, miR-1179, miR-3529-3p, miR-5011-5p as potential diagnostic biomarkers in isolated cervical dystonia. Rev. Neurol. (Paris). https://doi.org/10.1016/j.neurol.2022.10.008.

Gonzalez-Alegre, P., Paulson, H.L., 2004. Aberrant cellular behavior of mutant torsinA implicates nuclear envelope dysfunction in DYT1 dystonia. J. Neurosci. 24 (11), 2593–2601. https://doi.org/10.1523/JNEUROSCI.4461-03.2004.

Goodchild, R.E., Kim, C.E., Dauer, W.T., 2005. Loss of the dystonia-associated protein torsinA selectively disrupts the neuronal nuclear envelope. Neuron 48 (6), 923–932. https://doi.org/10.1016/j.neuron.2005.11.010.

Grundmann, K., Hubener, J., Habig, K., Reischmann, B., Poths, S., Hauser, T.K., Magg, J., Riess, O., Bonin, M., Nguyen, H.P., 2008. Gene expression changes in a transgenic mouse model overexpressing human wildtype and mutant torsinA. Proteomics Clin. Appl. 2 (5), 720–736. https://doi.org/10.1002/prca.200780053.

Hewett, J., Gonzalez-Agosti, C., Slater, D., Ziefer, P., Li, S., Bergeron, D., Jacoby, D.J., Ozelius, L.J., Ramesh, V., Breakefield, X.O., 2000. Mutant torsinA, responsible for early-onset torsion dystonia, forms membrane inclusions in cultured neural cells. Hum. Mol. Genet. 9 (9), 1403–1413. https://doi.org/10.1093/hmg/9.9.1403.

Humanes-Valera, D., Foffani, G., Aguilar, J., 2014. Increased cortical responses to forepaw stimuli immediately after peripheral deafferentation of hindpaw inputs. Sci. Rep. 4, 7278. https://doi.org/10.1038/srep07278.

Iacono, D., Geraci-Erck, M., Peng, H., Rabin, M.L., Kurlan, R., 2019. Hypertrophy of nigral neurons in Torsin1A deletion (DYT1) carriers manifesting dystonia. Parkinsonism Relat. Disord. 58, 63–69. https://doi.org/10.1016/j.parkreldis.2018.08.020.

Ip, C.W., Isaias, I.U., Kusche-Tekin, B.B., Klein, D., Groh, J., O'Leary, A., Knorr, S., Higuchi, T., Koprich, J.B., Brotchie, J.M., Toyka, K.V., Reif, A., Volkmann, J., 2016. Tor1a+/− mice develop dystonia-like movements via a striatal dopaminergic dysregulation triggered by peripheral nerve injury. Acta Neuropathol. Commun. 4 (1), 108. https://doi.org/10.1186/s40478-016-0375-7.

Jankovic, J., Van der Linden, C., 1988. Dystonia and tremor induced by peripheral trauma: predisposing factors. J. Neurol. Neurosurg. Psychiatry 51 (12), 1512–1519. https://doi.org/10.1136/jnnp.51.12.1512.

Jokhi, V., Ashley, J., Nunnari, J., Noma, A., Ito, N., Wakabayashi-Ito, N., Moore, M.J., Budnik, V., 2013. Torsin mediates primary envelopment of large ribonucleoprotein granules at the nuclear envelope. Cell Rep. 3 (4), 988–995. https://doi.org/10.1016/j.celrep.2013.03.015.

Kelleher 3rd, R.J., Govindarajan, A., Tonegawa, S., 2004. Translational regulatory mechanisms in persistent forms of synaptic plasticity. Neuron 44 (1), 59–73. https://doi.org/10.1016/j.neuron.2004.09.013.

Kelley, K., Lai, K., 2011. Accuracy in parameter estimation for the root mean square error of approximation: sample size planning for narrow confidence intervals. Multivar. Behav. Res. 46 (1), 1–32. https://doi.org/10.1080/00273171.2011.543027.

Klann, E., Antion, M.D., Banko, J.L., Hou, L., 2004. Synaptic plasticity and translation initiation. Learn. Mem. 11 (4), 365–372. https://doi.org/10.1101/lm.79004.

Knorr, S., Rauschenberger, L., Pasos, U.R., Friedrich, M.U., Peach, R.L., Grundmann-Hauser, K., Ott, T., O'Leary, A., Reif, A., Tovote, P., Volkmann, J., Ip, C.W., 2021. The evolution of dystonia-like movements in TOR1A rats after transient nerve injury is accompanied by dopaminergic dysregulation and abnormal oscillatory activity of a central motor network. Neurobiol. Dis. 154, 105337 https://doi.org/10.1016/j.nbd.2021.105337.

Kramer, P.L., Heiman, G.A., Gasser, T., Ozelius, L.J., de Leon, D., Brin, M.F., Burke, R.E., Hewett, J., Hunt, A.L., Moskowitz, C., et al., 1994. The DYT1 gene on 9q34 is responsible for most cases of early limb-onset idiopathic torsion dystonia in non-Jews. Am. J. Hum. Genet. 55 (3), 468–475. https://www.ncbi.nlm.nih.gov/pubmed/8079990.

Liu, Y., Xing, H., Sheng, W., Singh, K.N., Korkmaz, A.G., Comeau, C., Anika, M., Ernst, A., Yokoi, F., Vaillancourt, D.E., Frazier, C.J., Li, Y., 2021. Alteration of the cholinergic system and motor deficits in cholinergic neuron-specific Dyt1 knockout mice. Neurobiol. Dis. 154, 105342 https://doi.org/10.1016/j.nbd.2021.105342.

Macerollo, A., Edwards, M.J., Huang, H.C., Lu, M.K., Chen, H.J., Tsai, C.H., Chen, J.C., 2019. Peripheral trauma and risk of dystonia: what are the evidences and potential co-risk factors from a population insurance database? PLoS One 14 (5), e0216772. https://doi.org/10.1371/journal.pone.0216772.

Martella, G., Tassone, A., Sciamanna, G., Platania, P., Cuomo, D., Viscomi, M.T., Bonsi, P., Cacci, E., Biagioni, S., Usiello, A., Bernardi, G., Sharma, N., Standaert, D. G., Pisani, A., 2009. Impairment of bidirectional synaptic plasticity in the striatum of a mouse model of DYT1 dystonia: role of endogenous acetylcholine. Brain 132 (Pt 9), 2336–2349. https://doi.org/10.1093/brain/awp194.

Martin, J.N., Bair, T.B., Bode, N., Dauer, W.T., Gonzalez-Alegre, P., 2009. Transcriptional and proteomic profiling in a cellular model of DYT1 dystonia. Neuroscience 164 (2), 563–572. https://doi.org/10.1016/j.neuroscience.2009.07.068.

Mathis, A., Mamidanna, P., Cury, K.M., Abe, T., Murthy, V.N., Mathis, M.W., Bethge, M., 2018. DeepLabCut: markerless pose estimation of user-defined body parts with deep learning. Nat. Neurosci. 21 (9), 1281–1289. https://doi.org/10.1038/s41593-018-0209-y.

Menorca, R.M., Fussell, T.S., Elfar, J.C., 2013. Nerve physiology: mechanisms of injury and recovery. Hand Clin. 29 (3), 317–330. https://doi.org/10.1016/j.hcl.2013.04.002.

Mitchell, S.B., Chimenti, M.S., Kawano, H., Yuen, T.M.T., Sjurson, A.E., Iwabuchi, S., Knudtson, K.L., Bair, T.B., Kolbe, D., Harata, N.C., 2019. Transcriptome profiles in brains of mice heterozygous for a DYT1 dystonia-associated mutation in the endogenous *Tor1a* gene. bioRxiv 825505. https://doi.org/10.1101/825505.

Neychev, V.K., Fan, X., Mitev, V.I., Hess, E.J., Jinnah, H.A., 2008. The basal ganglia and cerebellum interact in the expression of dystonic movement. Brain 131 (Pt 9), 2499–2509. https://doi.org/10.1093/brain/awn168.

Niethammer, M., Carbon, M., Argyelan, M., Eidelberg, D., 2011. Hereditary dystonia as a neurodevelopmental circuit disorder: evidence from neuroimaging. Neurobiol. Dis. 42 (2), 202–209. https://doi.org/10.1016/j.nbd.2010.10.010.

Nieuwhof, F., Toni, I., Dirkx, M.F., Gallea, C., Vidailhet, M., Buijink, A.W.G., van Rootselaar, A.F., van de Warrenburg, B.P.C., Helmich, R.C., 2022. Cerebello-thalamic activity drives an abnormal motor network into dystonic tremor. Neuroimage Clin 33, 102919. https://doi.org/10.1016/j.nicl.2021.102919.

Park, C.Y., Choi, Y.S., McManus, M.T., 2010. Analysis of microRNA knockouts in mice. Hum. Mol. Genet. 19 (R2), R169–R175. https://doi.org/10.1093/hmg/ddq367.

Patil, A.H., Halushka, M.K., 2021. miRge3.0: a comprehensive microRNA and tRF sequencing analysis pipeline. NAR Genom Bioinform 3 (3), lqab068. https://doi.org/10.1093/nargab/lqab068.

Pizoli, C.E., Jinnah, H.A., Billingsley, M.L., Hess, E.J., 2002. Abnormal cerebellar signaling induces dystonia in mice. J. Neurosci. 22 (17), 7825–7833. https://doi.org/10.1523/JNEUROSCI.22-17-07825.2002.

Quartarone, A., Hallett, M., 2013. Emerging concepts in the physiological basis of dystonia. Mov. Disord. 28 (7), 958–967. https://doi.org/10.1002/mds.25532.

Quartarone, A., Bagnato, S., Rizzo, V., Siebner, H.R., Dattola, V., Scalfari, A., Morgante, F., Battaglia, F., Romano, M., Girlanda, P., 2003. Abnormal associative plasticity of the human motor cortex in writer's cramp. Brain 126 (Pt 12), 2586–2596. https://doi.org/10.1093/brain/awg273.

Rauschenberger, L., Knorr, S., Pisani, A., Hallett, M., Volkmann, J., Ip, C.W., 2021. Second hit hypothesis in dystonia: dysfunctional cross talk between neuroplasticity and environment? Neurobiol. Dis. 159, 105511 https://doi.org/10.1016/j.nbd.2021.105511.

Rauschenberger, L., Krenig, E.M., Stengl, A., Knorr, S., Harder, T.H., Steeg, F., Friedrich, M.U., Grundmann-Hauser, K., Volkmann, J., Ip, C.W., 2023. Peripheral nerve injury elicits microstructural and neurochemical changes in the striatum and substantia nigra of a DYT-TOR1A mouse model with dystonia-like movements. Neurobiol. Dis. 179, 106056 https://doi.org/10.1016/j.nbd.2023.106056.

Richter, J.D., 2001. Think globally, translate locally: what mitotic spindles and neuronal synapses have in common. Proc. Natl. Acad. Sci. USA 98 (13), 7069–7071. https://doi.org/10.1073/pnas.111146498.

Ritchie, M.E., Phipson, B., Wu, D., Hu, Y., Law, C.W., Shi, W., Smyth, G.K., 2015. Limma powers differential expression analyses for RNA-sequencing and microarray studies. Nucleic Acids Res. 43 (7), e47 https://doi.org/10.1093/nar/gkv007.

Rittiner, J.E., Caffall, Z.F., Hernandez-Martinez, R., Sanderson, S.M., Pearson, J.L., Tsukayama, K.K., Liu, A.Y., Xiao, C., Tracy, S., Shipman, M.K., Hickey, P., Johnson, J., Scott, B., Stacy, M., Saunders-Pullman, R., Bressman, S., Simonyan, K., Sharma, N., Ozelius, L.J., Calakos, N., 2016. Functional genomic analyses of Mendelian and sporadic disease identify impaired eIF2alpha signaling as a generalizable mechanism for dystonia. Neuron 92 (6), 1238–1251. https://doi.org/10.1016/j.neuron.2016.11.012.

Ru, Y., Kechris, K.J., Tabakoff, B., Hoffman, P., Radcliffe, R.A., Bowler, R., Mahaffey, S., Rossi, S., Calin, G.A., Bemis, L., Theodorescu, D., 2014. The multiMiR R package and database: integration of microRNA-target interactions along with their disease and drug associations. Nucleic Acids Res. 42 (17), e133 https://doi.org/10.1093/nar/gku631.

Shroff, K., Caffall, Z.F., Calakos, N., 2021. DYT-TOR1A subcellular proteomics reveals selective vulnerability of the nuclear proteome to cell stress. Neurobiol. Dis. 158, 105464 https://doi.org/10.1016/j.nbd.2021.105464.

Smith, C.E., Cribbie, R.A., 2013. Multiplicity control in structural equation modeling: incorporating parameter dependencies. Struct. Equ. Model. Multidiscip. J. 20 (1), 79–85. https://doi.org/10.1080/10705511.2013.742385.

Song, C.H., Bernhard, D., Hess, E.J., Jinnah, H.A., 2014. Subtle microstructural changes of the cerebellum in a knock-in mouse model of DYT1 dystonia. Neurobiol. Dis. 62, 372–380. https://doi.org/10.1016/j.nbd.2013.10.003.

Tassone, A., Martella, G., Meringolo, M., Vanni, V., Sciamanna, G., Ponterio, G., Imbriani, P., Bonsi, P., Pisani, A., 2021. Vesicular acetylcholine transporter alters cholinergic tone and synaptic plasticity in DYT1 dystonia. Mov. Disord. 36 (12), 2768–2779. https://doi.org/10.1002/mds.28698.

Thelen, M.P., Kye, M.J., 2019. The role of RNA binding proteins for local mRNA translation: implications in neurological disorders. Front. Mol. Biosci. 6, 161. https://doi.org/10.3389/fmolb.2019.00161.

Turakhiya, A., Meyer, S.R., Marincola, G., Bohm, S., Vanselow, J.T., Schlosser, A., Hofmann, K., Buchberger, A., 2018. ZFAND1 recruits p97 and the 26S proteasome to promote the clearance of Arsenite-induced stress granules. Mol. Cell 70 (5), 906–919 e907. https://doi.org/10.1016/j.molcel.2018.04.021.

Ueta, Y., Miyata, M., 2021. Brainstem local microglia induce whisker map plasticity in the thalamus after peripheral nerve injury. Cell Rep. 34 (10), 108823 https://doi.org/10.1016/j.celrep.2021.108823.

Vasudevan, A., Breakefield, X.O., Bhide, P.G., 2006. Developmental patterns of torsinA and torsinB expression. Brain Res. 1073-1074, 139–145. https://doi.org/10.1016/j.brainres.2005.12.087.

Yokoi, F., Dang, M.T., Liu, J., Gandre, J.R., Kwon, K., Yuen, R., Li, Y., 2015. Decreased dopamine receptor 1 activity and impaired motor-skill transfer in Dyt1 DeltaGAG heterozygous knock-in mice. Behav. Brain Res. 279, 202–210. https://doi.org/10.1016/j.bbr.2014.11.037.

Yu, G., Wang, L.G., Han, Y., He, Q.Y., 2012. clusterProfiler: an R package for comparing biological themes among gene clusters. OMICS 16 (5), 284–287. https://doi.org/10.1089/omi.2011.0118.